PNAS
www.pnas.org

Supplementary Information for

Programming curvilinear paths of flat inflatables

Emmanuel Siéfert, Etienne Reyssat, José Bico, Benoît Roman

Emmanuel Siéfert.
E-mail: emmanuel.siefert@espci.fr

This PDF file includes:

> Supplementary text
> Figs. S1 to S4
> Captions for Movies S1 to S5
> References for SI reference citations

Other supplementary materials for this manuscript include the following:

> Movies S1 to S5

Supporting Information Text

A. Derivation of the equations based on volume maximization. We consider two superposed flat rings, sealed on their edges, of inner radius R and outer radius $R + w$. We assume that when inflated, the membrane is inextensible, but that, being infinitely bendable, it may freely accomodate excess of material with wrinkles. We are interested in the resulting inflated overall shape (and not on the detail of the morphology of the wrinkles). This surface is assumed to remain axisymmetric, with the inextensible meridian always under tension, whereas azimuthal compression could occur on this surface (by forming wrinkles in the actual membrane).

The section of the torus is described by the curvilinear coordinate s along a meridian, the vertical coordinate $z(s)$, the radial coordinate $R + r(s)$, and the angle φ of the tangent to the meridian line with respect to $\mathbf{e_r}$ (Fig S1A). The shape of the section is assumed to be symmetrical with respect to the $\mathbf{e_r}$ axis. In this framework, the equilibrium shape corresponds to the shape which minimizes the energy $U = -pV$, or equivalently, which maximizes the volume V of the toroidal shape obtained by rotational symmetry (1). The volume reads

$$V = 4\pi \int_0^w [R + r(s)]z(s)\cos\varphi \, \mathrm{d}s \tag{1}$$

In the radial direction, inextensibility is simply ensured by the limits of the integral, because we assume that meridians are not wrinkled *i.e.* that the membrane is not compressed anywhere in the radial direction. In the azimuthal direction, inextensibility imposes the following inequality

$$\forall s, P(s) \leq P^0(s), \tag{2}$$

where we have defined the apparent perimeter $P(s) = 2\pi(R + r(s))$ of the circle passing through a point s of the section, and $P^0(s) = 2\pi(R + s)$ its initial perimeter. Here this continuous inequality can be greatly simplified in the following way : the radial inextensibility imposes that $\forall s, r'(s) = \cos\varphi \leq 1$, and thus $P'(s) \leq P^{0'}(s)$. Therefore Eq.[2] is satisfied if and only if $P(0) \leq P^0(0)$, or equivalently if and only if $r(0) \leq 0$. An optimal solution must equalize the inequality constraint for at least one curvilinear coordinate, and from the previous equation it must be at $s = 0$. The inextensibility condition [2] thus reduces to the boundary condition:

$$r(0) = 0 \tag{3}$$

Dividing lengths by w, the Lagrangian for the optimization problem may be written in terms of non-dimensional variables and parameters denoted by *. We choose here $z(s)$, $r(s)$, and $\varphi(s)$ as independent functions for our optimization problem, for the sake of computation simplicity. The problem is now to maximize

$$\int_0^1 \left[(R^* + r^*)z^*\cos\varphi + A(\cos\varphi - r^{*\prime}) + B(\sin\varphi - z^{*\prime}) \right] \mathrm{d}s^*, \tag{4}$$

where $(')$ stands for derivatives with respect to s^*. A and B are two Lagrange multipliers enforcing the geometrical relations $(r^{*\prime} = \cos\varphi; z^{*\prime} = \sin\varphi)$, that we shall interpret later. Using classical variational methods, we get the following system of equations for the maximization :

$$\begin{cases} A' = -z^*\cos\varphi \\ B' = -(R^* + r^*)\cos\varphi \\ r^{*\prime} = \cos\varphi \\ z^{*\prime} = \sin\varphi \\ [A + z^*(R^* + r^*)]\sin\varphi = B\cos\varphi \end{cases} \tag{5}$$

together with the boundary conditions $A(1) = 0$ because $r^*(0) = 0$ is fixed as seen above (equation [3]), whereas $r^*(1)$ is free. We also have the boundary conditions $z^*(0) = z^*(1) = 0$ from symmetry. We do have the four needed boundary conditions to solve the system of four first order ODEs. It is however interesting to show that these equations are equivalent to equations [1,2] of the main article and related boundary conditions.

Differentiating the last equation in the set of equation [5] and using the other relations to simplify, one gets the equation:

$$\frac{\mathrm{d}\varphi}{\mathrm{d}s} = -\frac{(R + r)\sin\varphi}{B} \tag{6}$$

It can be easily shown by direct differentiation that the quantity $\sin\varphi/B$ is a constant (using again [5] and [6]). Hence equation [6] shows that $d\varphi/ds$ is strictly proportional to $(R + r)$, and we have recovered equation [1] of the main part of the article where the constant $\sin\varphi/B$ corresponds in physical terms to p/C.

The boundary conditions may also be expressed as function of $\varphi(s)$. $z^*(0) = z^*(1) = 0$ simply imposes that $\int_0^1 \sin\varphi \mathrm{d}s^* = 0$, and the condition $r^*(0) = 0$ inserted in [6] leads to

$$\varphi'(0) = -pR/C$$

Finally, evaluating the last equation in the set of equation [5] at $s^* = 1$, and knowing that $B = C/p\sin\varphi$, $z^*(1) = 0$ and $A(1) = 0$, we obtain that

$$\varphi(1) = -\pi/2.$$

**Emmanuel Siéfert, Etienne Reyssat, José Bico, Benoît Roman**

We may also interpret Lagrange parameters A and B that appear in the variational equations by separating an angular sector of the system with an imaginary cylindrical cut of radius $R + r_0$ and considering the force exerted by the portion $r > r_0$ on the part $r < r_0$ (see Supplementary Fig. S1B). A and B are simply the horizontal and vertical projection of this force.

$$B = C/p \sin \varphi, \qquad [7]$$

is the vertical projection of the dimensionless membrane tension per unit angular sector. The total dimensionless horizontal force

$$A = C/p \cos \varphi - z^* \qquad [8]$$

also includes a contribution of the pressure on the section in addition to the projected membrane tension.
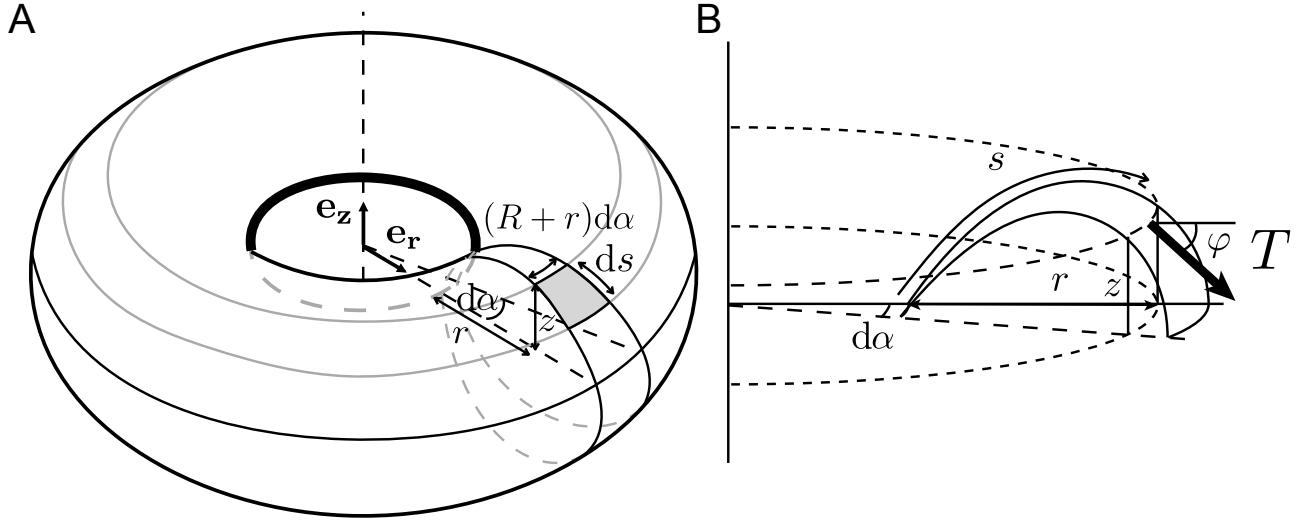

Fig. S1. (A)-(B) Schetch of the inflated toroidal shape with the definition of parameter s, r, z, φ and the tension T. In (B) the intersection between a angular sector $\mathrm{d}\alpha$ and a cylinder of radius $R + r$ is shown for the interpretation of the Lagrangian parameters A and B

B. Results interpretation. We can solve this boundary value problem using Matlab function bvp4c varying the only non dimensional parameter of the system, the ratio inner over outer radius $R^*/(R^* + 1)$ and compare the results with cross sections measured experimentally (see Fig. 3B in the main manuscript). The theoretical predictions (solid lines) are in remarkable quantitative agreement with the experimental measurements (triangles). For slender rings, that is when $R^*/(R^* + 1) \to 1$, the cross-section tends to the trivial cross-section of a straight inflated path, a circle. However, when $R^*/(R^* + 1) \to 0$, the cross-section strongly deviates from a circle and a singularity appears at the inner point $s^* = 0$. One intuitive way to grasp the idea of this shape is the following: the volume of a toroidal shape is the product of the area of the cross section times the length OC from the center of symmetry (O) of the torus to the centroid (C) of the cross-section. When the ring is highly slender, $R^* \gg 1$, the length $OC \in [R^*, R^* + 1]$ is nearly independent of the cross section. The volume optimization reduces thus to the legendary problem of Queen Dido of Carthage, that is, maximizing a surface given a fixed perimeter length, a circle. However, when $R^* \to 0$ ($OC \in [0, 1]$), the position of the centroid is crucial for the volume optimization problem: the system pays a loss in the area of the cross-section in order to push the centroid away from (O), leading to this asymmetric cross-section shape.

C. Open rings. Inflating such objects with one more degree of freedom, we observe that they remain in-plane, but that the curvature of their outline tends to increase (see Fig.3A of the main text). The open-end condition now allows for an overlapping angle $\Delta \alpha$ to be determined. The previous expression [1] for the volume V is only modified into $(1 + \epsilon_\alpha)V$, where we have noted $\epsilon_\alpha = \Delta \alpha / 2\pi$. We may use the modified Lagrangian $(1 + \epsilon_\alpha)L$ in the minimization, and recover the same set of equations [4]. However the perimeters now include overlapping portions of circles with total length $P_{\epsilon_\alpha}(s) = 2\pi(R + (1 + \epsilon_\alpha)r(s))$. The inextensible boundary condition for the inner line now imposes $R_1 = R/(1 + \epsilon_\alpha)$. We see that the value of the strain ϵ_α determines the radius of the curvature of the inner circle and the shape of the section (within the previously calculated family). Finally the free parameter ϵ_α may be determined by maximizing the corresponding volume $V(\epsilon_\alpha)$, provided the sections obey the inextensibility condition (2) for each of their points.

The volume is numerically found to be an increasing function of ϵ_α. The optimal solution is thus expected to have the maximum ϵ_α that satisfies the inextensibility condition (2), which is shown in Fig. 4B of the main document.
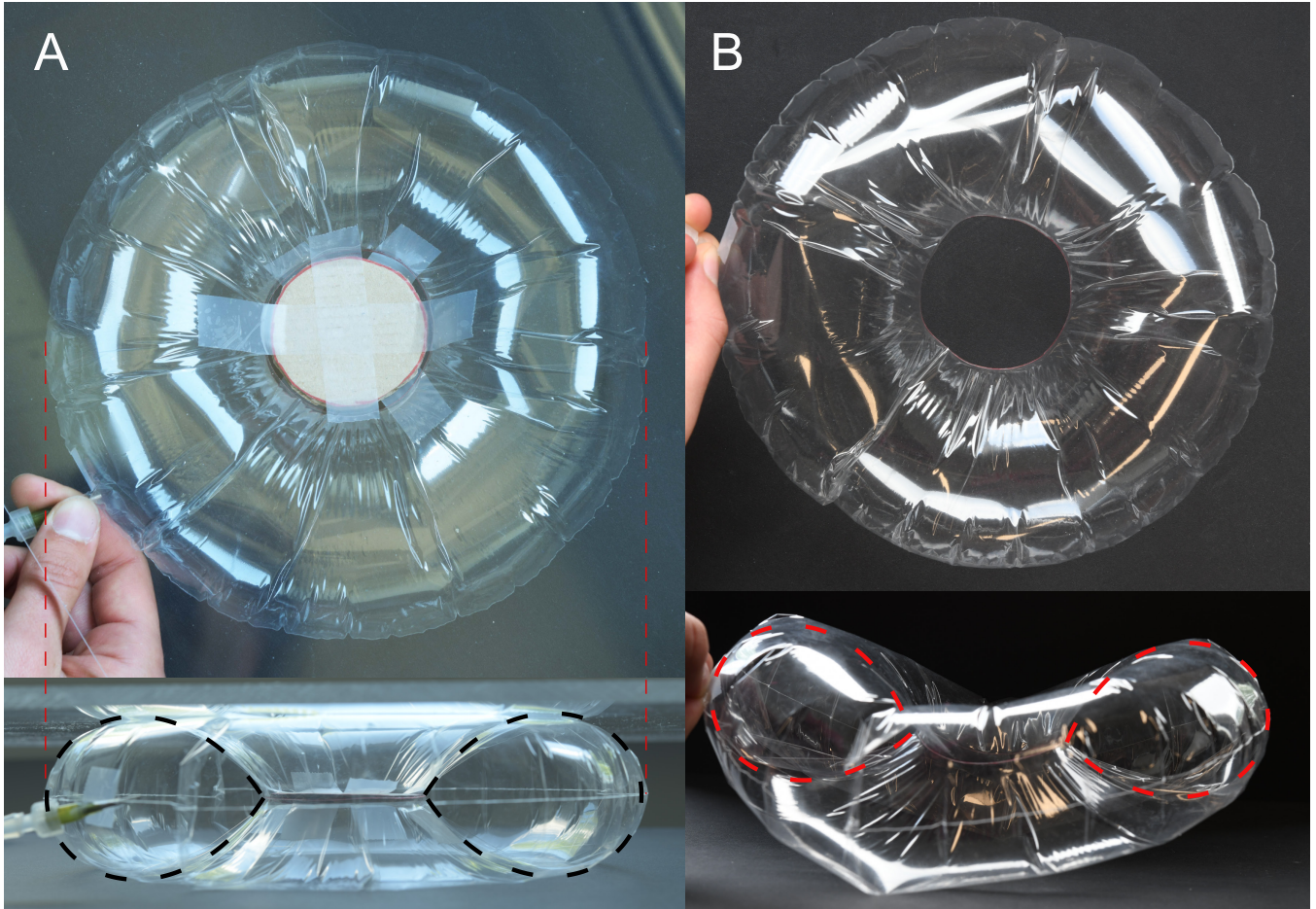
Fig. S2. Pictures of (A) constrained and (B) unconstrained inflated annuli. (A) The toroidal shape is constrained to remain in plane by two parallel plates with a controlled gap. (B) The same object freely buckles out of plane when the constraint is released. However, the cross sections barely evolves and match the theoretical prediction in dashed line.

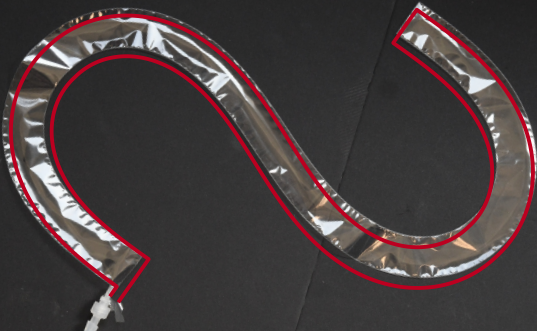**Emmanuel Siéfert, Etienne Reyssat, José Bico, Benoît Roman**

Fig. S3. Pictures of the same commercial mylar balloon before (left) and after (right) inflation. The letter, which looks like a "C" in the rest state, coils onto an "O" upon inflation.
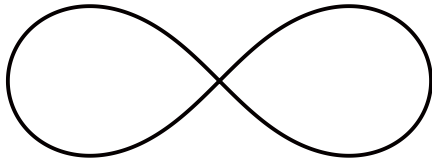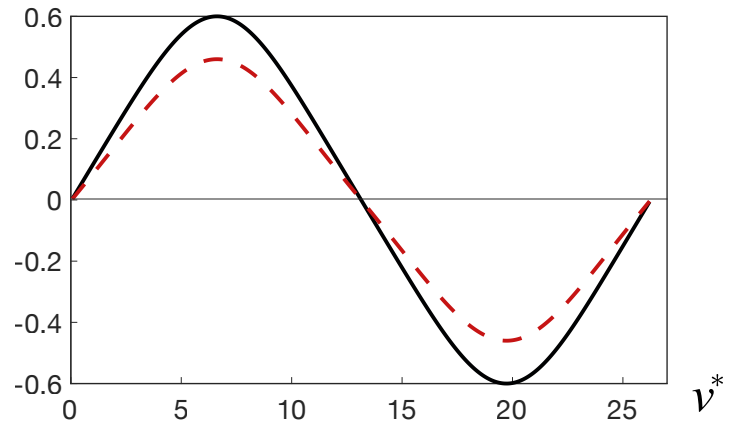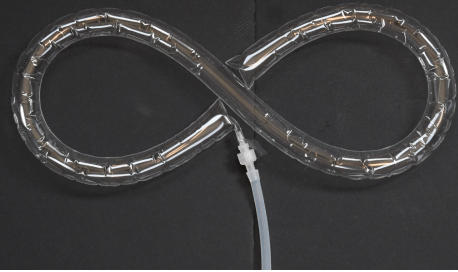
Fig. S4. Programming of a lemniscate. (A) Target outline, (B) normalized curvature of the lemniscate κ_{tar} and of the fabrication state $1/R^*$, computed using equation [5] in the main article. The corresponding pattern on top of a picture of the structure in the flat state is shown in (C). (D) Upon inflation, the structure coils into the target lemniscate outline.

Emmanuel Siéfert, Etienne Reyssat, José Bico, Benoît Roman

Movie S1. Inflation of a flat closed ring. The inflated structure surprisingly buckles out of plane. The ring (inner radius $R = 85mm$ and width $w = 51mm$) is made of TPU coated Ripstop nylon fabric $20den$, from Extremtextil.

Movie S2. Inflation of a flat open ring. The inflated structure overcurves and exhibits an excess angle. The ring (inner radius $R = 60mm$ and width $w = 17mm$) is made of TPU coated Ripstop nylon fabric $20den$, from Extremtextil.

Movie S3. Programming of a "waving man". Upon inflation, the flat sealed path is programmed to shape the contour of a waving man. The structure (of width $w = 1.5mm$) is made of a polypropylene sheet of thickness $t = 16\mu m$.

Movie S4. Programming "hello". Upon inflation, the flat sealed path is programmed to shape the handwritten "hello". The structure (of width $w = 1.2mm$) is made of a polypropylene sheet of thickness $t = 16\mu m$.

Movie S5. Manipulation of a mug. Upon inflation, the flat sealed arm deforms along a predicted path, passing an obstacle to carry and drop the mug on a platform. The arm is made of TPU coated nylon fabric $210den$ from Extremtextil.

References

1. Paulsen W (1994) What is the shape of a mylar balloon? *The American mathematical monthly* 101(10):953–958.